LIGHTWEIGHT SILVER INK PRINTED CIRCULAR RING MICROSTRIP PATCH ANTENNA FOR WLAN APPLICATIONS

by

Bobak Beheshti

Senior Project

ELECTRICAL ENGINEERING DEPARTMENT

California Polytechnic State University

San Luis Obispo

2015

TABLE OF CONTENTS

LIST OF TABLES

LIST OF FIGURES

ABSTRACT

Wireless communications systems include the internet, mobile phones, navigation, public safety and industrial processes. Many of these applications are managed under IEEE 802.11 WLAN (wireless local area network) protocols. WLAN connects communication devices over a short range (< 100m) and includes 2.4-5GHz bands.

This paper presents a probe fed planar microstrip patch antenna design for 2.4-5GHz WLAN applications. Compact and lightweight antennas are favored for applications involving portable electronics such as laptops. Directional antennas receive stronger signals from a signal source at a known location, e.g. a laptop antenna and a router, than omnidirectional antennas. A planar microstrip patch antenna is directional (between 5dB and 8dB) and can be flush mounted on flat surfaces. Developing patch antennas with exceptionally thin (< 0.003λ) substrates allow users to mount a lighter, more compact antenna to many portable devices. However, exceptionally thin substrates (thickness $h < 0.003\lambda$) decrease impedance bandwidth.

Circular ring patch antennas exhibit up to twice the impedance bandwidth of similarly sized generic rectangular patch antennas. A circular ring patch is designed for 2.4GHz operation with inner and outer radii of 1.090" and 2.320", respectively. DGS (defected ground structure), formed by partially removing the ground plane, widens impedance bandwidth by increasing ground plane current distribution and decreasing shielding to increase electromagnetic wave propagation in the substrate. A 1mm radius circular ring DGS is formed by removing the ground plane around the probe feed location, yielding an UWB (ultra-wideband) receiving antenna.

The circular ring patch is modeled using Ansys HFSS (High Frequency Structural Simulator). The patch is screen printed using conductive silver ink, a process performed in the Cal Poly Graphic Communications Special Resources Laboratory, and the ground plane is constructed with copper adhesive tape to afford relative ease of creating and modifying the DGS. The Cal Poly Electrical Engineering Department's Microwave Laboratory and anechoic chamber with vector network analyzers and Labview AMS (Antenna Measurement System) software are used for antenna testing.

The fabricated antenna achieves a 20dB return loss bandwidth from 2.313-5.550GHz, wider than the target 2.4-5GHz bandwidth. The simulated radiation pattern at 2.4GHz has maximum 5.7dB directivity above the patch and 1.4dB directivity below. The fabricated patch antenna's radiation pattern above the patch has maximum 7.1dB directivity, an improvement relative to the simulation.

I. INTRODUCTION

Table I: WLAN Operating Frequency Ranges and Applications

Frequency (GHz)	Description
2.412-2.462	802.11b/g/n; Wi-Fi internet, Bluetooth, Zigbee, majority of consumer applications.
3.658 -3.693	802.11a; Industrial controls.
5.180-5.825	802.11a/ac/n; Public safety resources, additional bandwidth for 2.4GHz applications.

Table I lists IEEE 802.11 WLAN operating frequency ranges requiring less than 100m distance range at low power [1]. The 2.4GHz band is used for internet, Bluetooth and Zigbee. Bluetooth enables communication between mobile phones or computers to peripheral devices, automatic device synchronization and home controls. Zigbee uses wireless networks in which all nodes are utilized to relay information and in home and building controls. The 3.7GHz band is reserved for industrial controls such as industrial Bluetooth and Zigbee. Industrial Bluetooth automates manufacturing and connects manufacturing facility sectors to remote locations and industrial Zigbee self-guides vehicles, monitors energy and connects proprietary radios for industrial equipment communication. The 5GHz frequency band allocates 5.180-5.825GHz for 2.4GHz Wi-Fi applications and enables public safety applications such as surveillance, emergency communications and security networks.

Many of these WLAN applications are mobile. A portable, mountable and directional antenna with low power consumption is favorable. Planar microstrip patch antennas fulfill the criteria listed. Patch antennas include two planar conductive materials, a radiating patch on top and ground plane underneath, separated by a dielectric substrate. Figure 1 and Figure 2 display a probe fed planar microstrip patch antenna's top and bottom views respectively. Figure 1 shows the radiating ring patch on a substrate with a probe feed. Figure 2 shows the ground plane and coaxial probe feed with a concentric annular ground defect around the probe feed. Figure 3 shows the coaxial probe feed's outer and inner conductors, connected to the ground and patch respectively depicted as cylinders connected to the top patch on the left patch antenna and bottom ground plane on the right patch antenna.

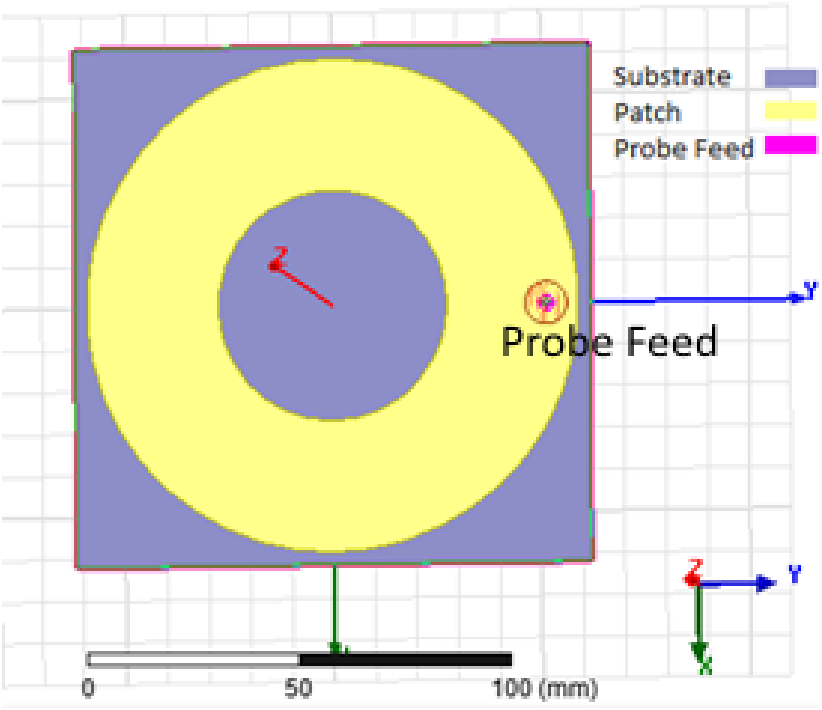

Figure 1: HFSS Circular Ring Patch Antenna Model, Radii = 27.9mm and 59mm, Copper Substrate, Silver Patch (Top View)

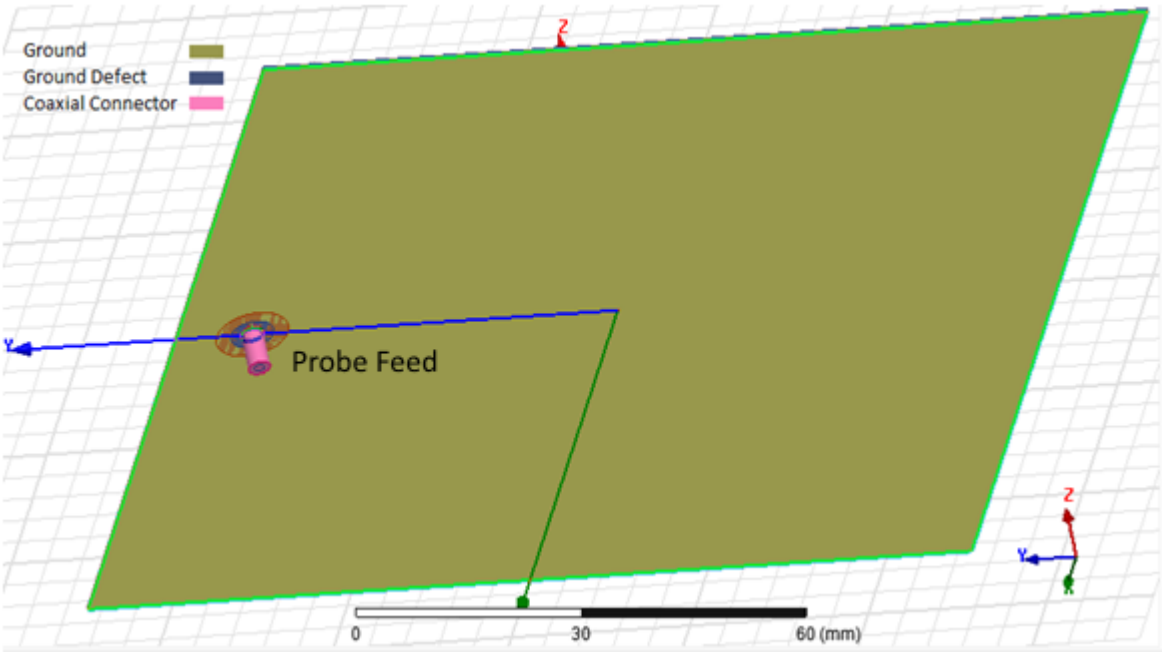

Figure 2: HFSS Circular Ring Patch Antenna Model, Length and Width = 123.9mm (Bottom View)

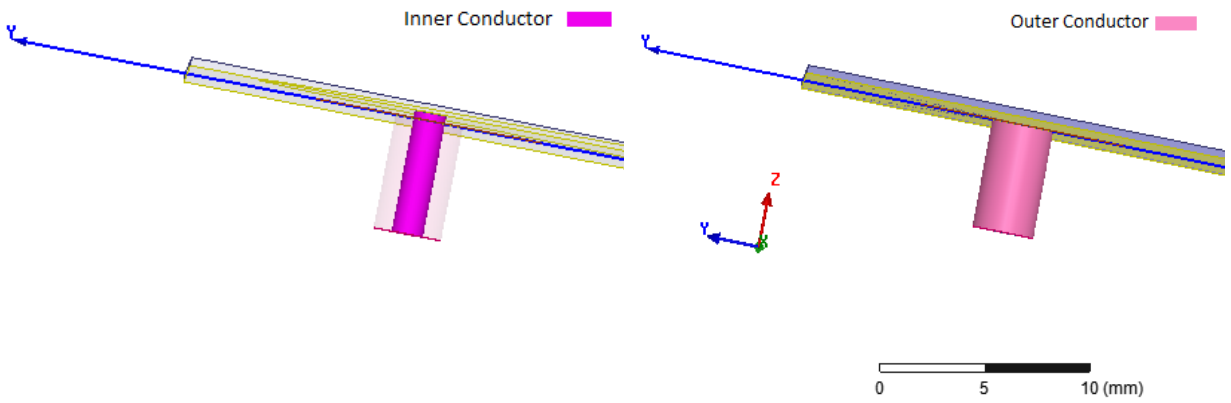

Figure 3: HFSS Circular Ring Patch Antenna Model (Side View) Inner Conductor to Patch (Left) and Outer Conductor to Ground (Right)

The typical patch antenna substrate thickness h is between 0.003λ and 0.050λ (15mil to 246mil at 2.4GHz). A patch antenna for which $h < 0.003\lambda$ is considered an electrically thin antenna. Decreasing substrate thickness h decreases percentage bandwidth $\%BW$ as follows, where w and l are patch antenna width and length respectively and A is the proportionality constant:

$$\%BW = \frac{Ah}{\lambda_0\sqrt{\varepsilon_r}}\sqrt{\frac{w}{l}} \quad (1)$$

Equation (1) expresses direct proportionality between h and $\%BW$ and Table II shows possible values of A in terms of other factors in (1) [2]:

Table II: Circular Ring Patch Antenna Percentage Bandwidth Relative Factors

$\frac{h}{\lambda_0\sqrt{\varepsilon_r}}$	A
≤ 0.045	180
≤ 0.075	200
≥ 0.075	220

The patch is printed on 14mils thick 100% PET (polyethylene terephthalate), a lightweight plastic ($\varepsilon_r = 3.2$). Equation (1) demonstrates that the use of a thin substrate necessitates design approaches which focus on impedance bandwidth improvement.

Bergman and Schultz originally proposed the popular circular ring patch antenna in 1955 as a wideband radiator [3]. DGS, created by deliberately removing a portion of the ground plane and exposing the substrate, widens impedance bandwidth by breaking ground plane current shielding, resulting in the excitation of electromagnetic waves. DGS reportedly achieves UWB performance and can potentially access all 2.4-5GHz WLAN frequency bands [4].

II. SYSTEM REQUIREMENTS AND SPECIFICATIONS

Table III: Circular Ring Patch Antenna Specifications

Specifications	Justification
Substrate height $h < 0.003\lambda$	Substrate is thinner than typical patch antenna substrates.
Nominal 50Ω driving point impedance	Impedance is matched to 50Ω coaxial connector.
Minimum 20dB return loss from 2.4-5GHz	Operating bandwidth includes 2.4-5GHz WLAN frequency bands.
Directional radiation pattern: 5dB < D_{dB} < 8dB toward user direction	Portable applications receive stronger radiation directed towards the user. Typical patch antennas exhibit between 5dB and 8dB directivity [5].
HPBW (H-plane): $\varphi_{HP} < 360°$	Omnidirectional in H-plane.
HPBW (E-plane): $18.205° < \theta_{HP} < 36.237°$	$D = \frac{41{,}253}{\theta_{HP}\varphi_{HP}}$ (2) $3.162 < D < 6.310$ Equation (2) relates directivity to HPBW (E-plane) [5].

Table III summarizes project specifications. D_{dB} is the main lobe (directional part of radiation pattern containing max radiated power) max directivity (max power density in direction of max radiated power). HPBW (half-power beamwidth) is the angular separation between two points where power measures 3dB lower than the max radiated power.

III. SYSTEM DESIGN AND ANALYSIS

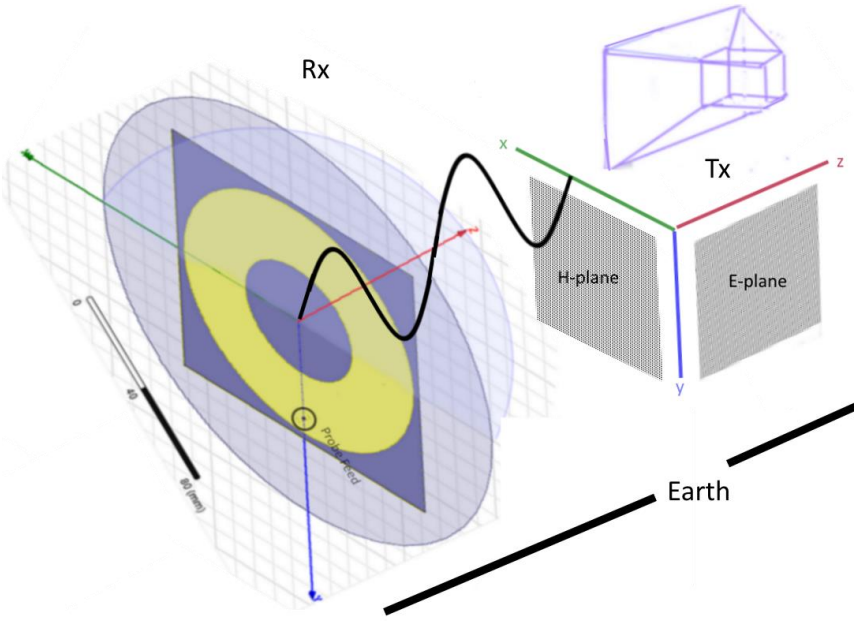

Figure 4: Receiving Circular Ring Patch and Transmitting Horn Antenna Co-Pol Test Setup

Figure 4 illustrates the vertically polarized antenna under test and E-plane (YZ) and H-plane (XZ). A broadband, directional and linearly polarized horn antenna transmits. The circular ring patch antenna's y-axis aligned probe feed results in the corresponding E-plane orientation.

Table IV: Circular Ring Patch Antenna Design Parameters

Parameter	Value	Description
f_{11}	2.4GHz	Resonant frequency for dominant TM_{11} mode
ε_r	3.2	PET dielectric constant

$$f_{mn} = \frac{X\prime_{mn}c}{2\pi r_i} \tag{3}$$

$$r_i = \frac{1.841c}{2\pi f_{11}\sqrt{\varepsilon_r}} = 20.460mm \tag{4}$$

$$0.350 > \frac{r_o - r_i}{r_o + r_i} \rightarrow r_o < 42.490mm \tag{5}$$

Table IV defines design parameters for a PET substrate at 2.4GHz resonant frequency. Equation (3) defines TM_{mn} mode circular ring patch resonant frequencies based on the uniform circular loop patch cavity model [6]. X'_{mn} is the zero of the m^{th} derivative Bessel function $J_m(x)$ for mode TM_{mn}, c is the speed of light in a vacuum and r_i and r_o are the circular ring patch inner and outer radius. Equations (4) and (5) define conductive patch inner and outer radii, respectively, assuming dominant TM_{11} mode [3]. HFSS optimization indicates greatest return loss occurs using r_i = 27.600mm (4.53λ and circumference 173.410mm) with outer radius r_o = 59.000mm (2.120λ and circumference 370.700mm). Probe feed radius and center HFSS optimization determines the probe feed location at (0.000mm, 51.200mm, 0.000mm). Table IV lists antenna width and height *RSize*, antenna thickness *ZSize* and probe feed and circular ring patch inner and outer radii *Radius*.

Table V: HFSS Circular Ring Patch Antenna Physical Dimensions

Structure	RSize [mm]	ZSize [mm]	Radius [mm]	Center (X, Y, Z) [mm]
Inner Ring	-	-	27.600	0.000, 0.000, 0.000
Outer Ring	-	-	59.000	0.000, 0.000, 0.000
Substrate	123.900	0.360	-	0.000, 0.000, 0.000
Ground	123.900	0.000	-	0.000, 0.000, 0.000
Probe Feed	-	0.360	0.700	0.000, 51.200, 0.000

Table VI: HFSS Circular Ring Patch Antenna Electrical Dimensions

Structure	RSize [λ]	ZSize [λ]	Radius [λ]	Center (X, Y, Z) [λ]
Inner Ring	-	-	4.530	0.000, 0.000, 0.000
Outer Ring	-	-	2.120	0.000, 0.000, 0.000
Substrate	1.010	351.500	-	0.000, 0.000, 0.000
Ground	1.010	0.000	-	0.000, 0.000, 0.000
Probe Feed	-	351.500	178.600	0.000, 2.440, 0.000

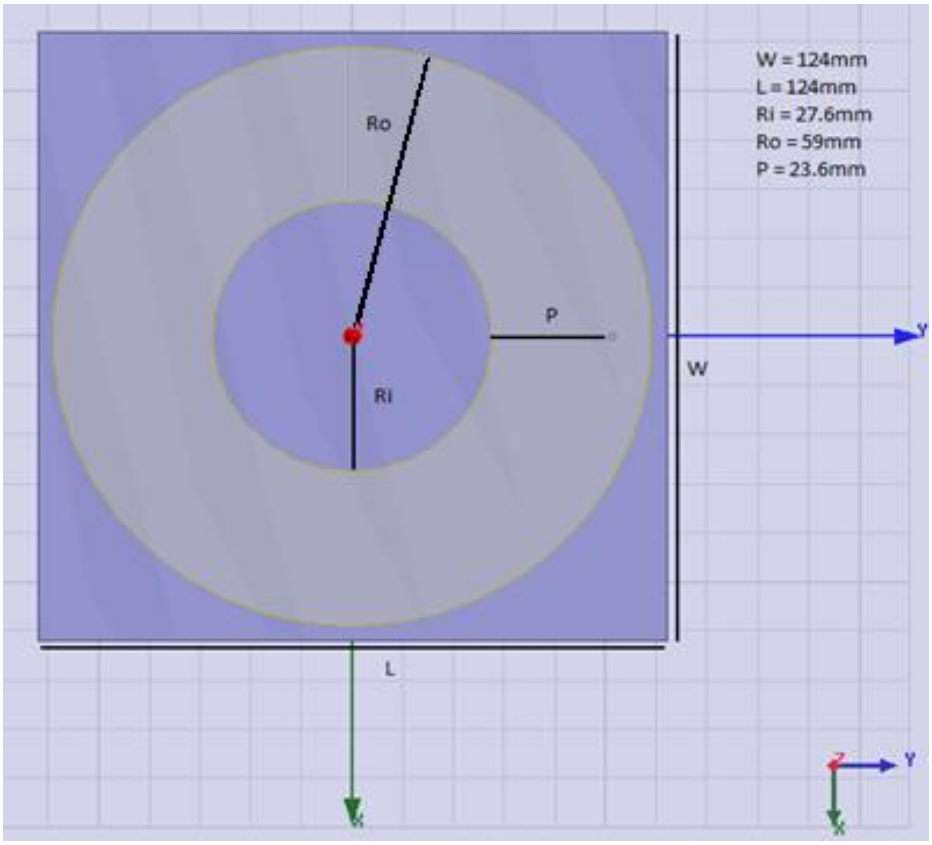

Figure 5: HFSS Circular Ring Patch Antenna Model (Top View)

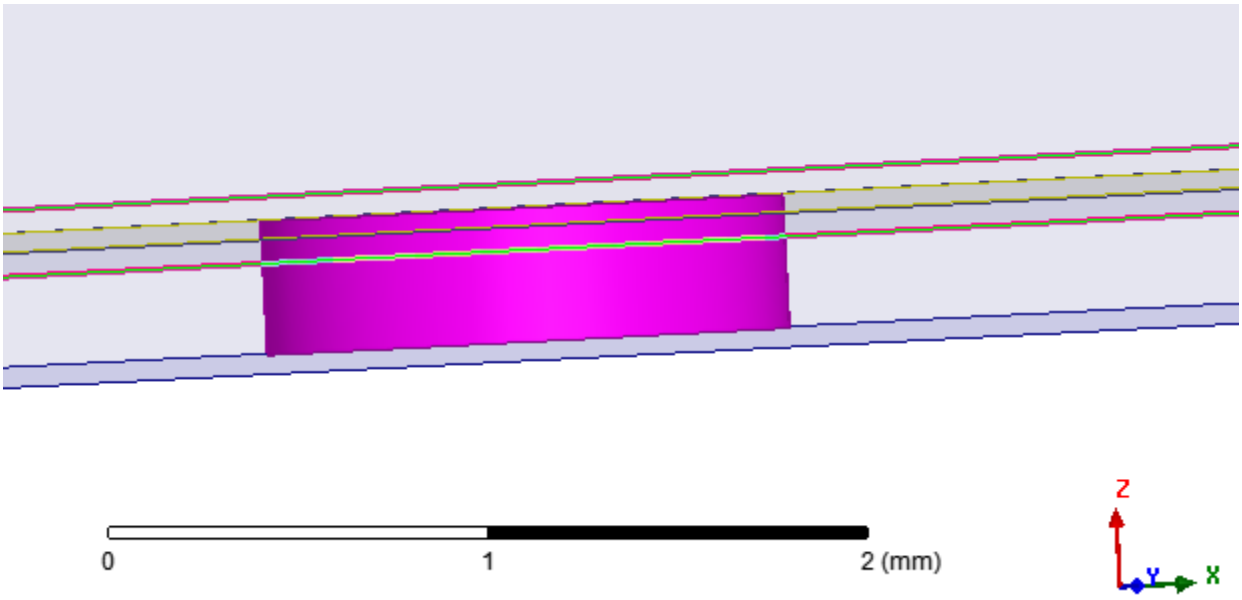

Figure 6: HFSS Circular Ring Patch Antenna Model Probe Feed

Tables V and VI summarize HFSS specifications. Figure 5 shows the HFSS patch antenna model top view with coordinate axes. Figure 6 shows the *Probe Feed* within the substrate.

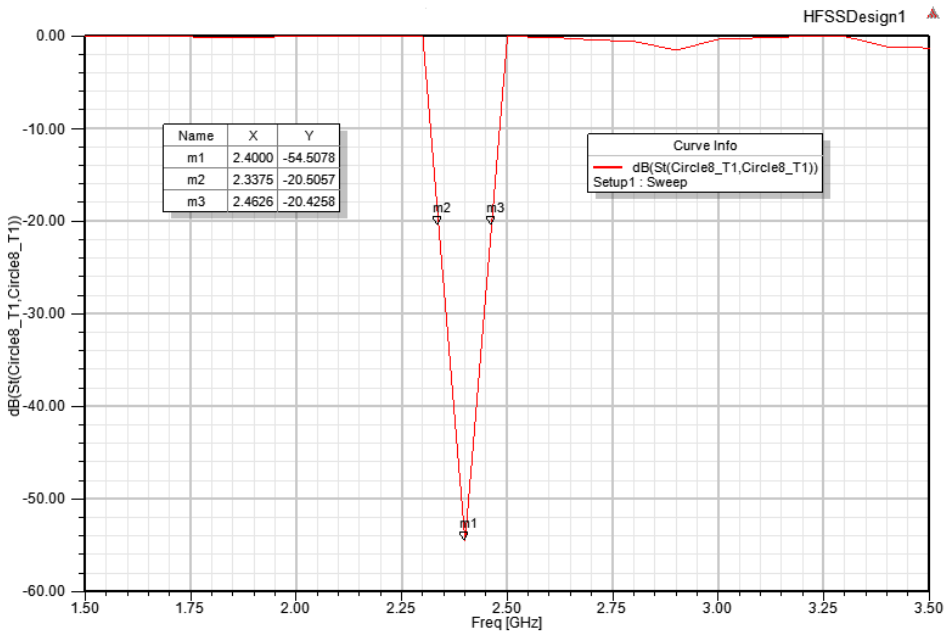

Figure 7: HFSS Circular Ring Patch Antenna $|S_{11}|$ (dB) vs. Frequency (GHz) without DGS

Figure 7 shows $|S_{11}|$ vs. frequency from 1.5GHz to 3.5GHz without DGS. Return loss simulations verify 54.508dB 50Ω impedance matching at the 2.4GHz resonant frequency.

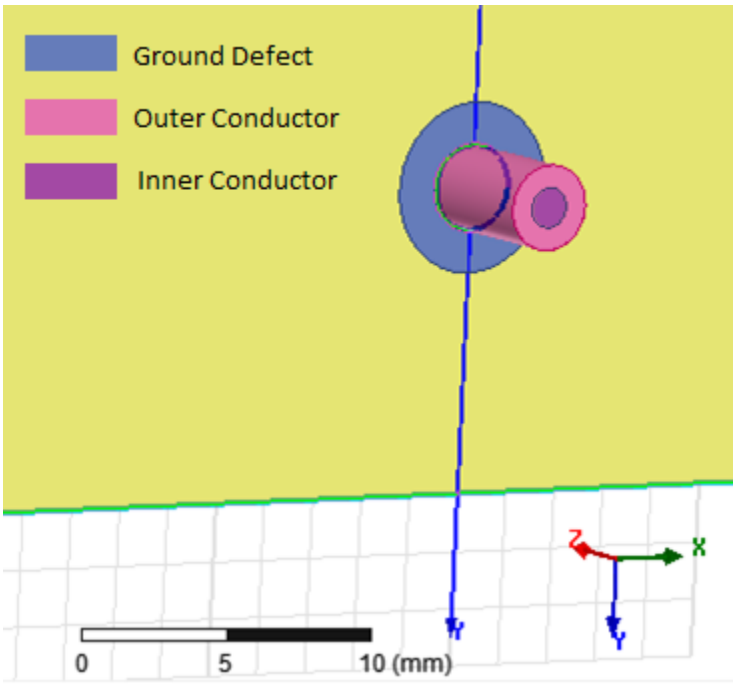

Figure 8: HFSS Circular Ring Patch Antenna Model with DGS

Figure 8 shows the simulated 1mm radius annular ground defect's location on the ground plane. The coaxial inner and outer conductors connect to the patch and ground plane, respectively.

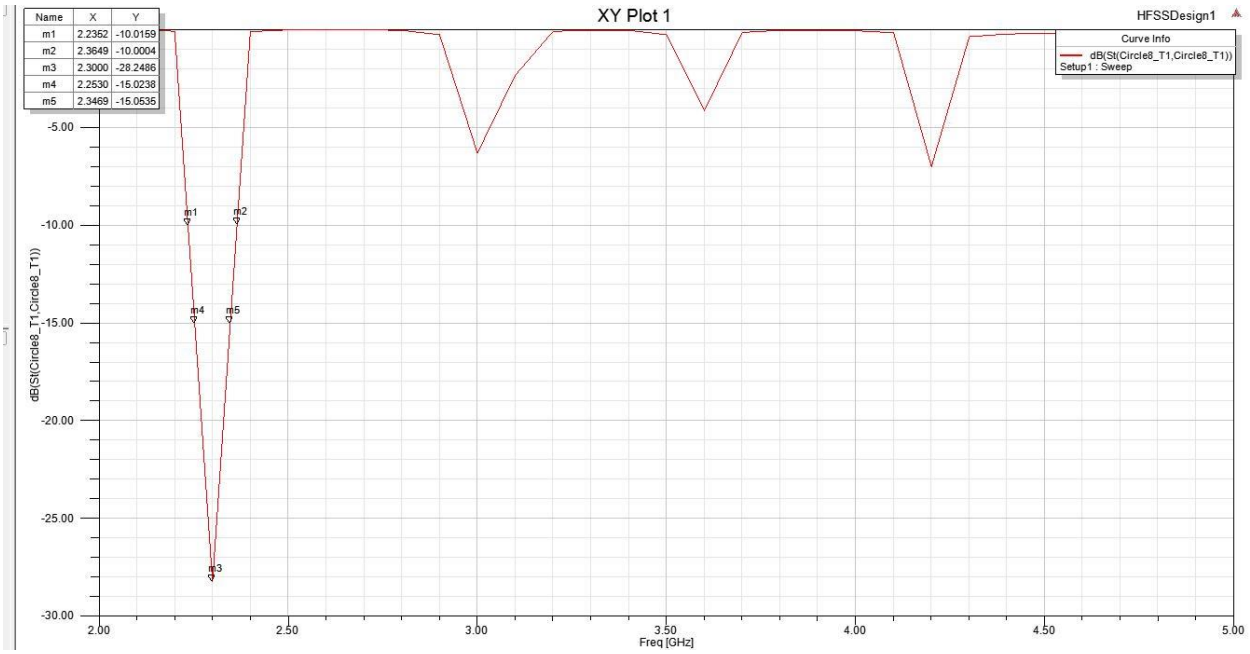

Figure 9: HFSS Circular Ring Patch Antenna $|S_{11}|$ (dB) vs. Frequency (GHz) with DGS

Figure 9 demonstrates the effect of a 1mm radius annular ground defect centered at the probe feed position and shows that resonance shifts from 2.4GHz to 2.3GHz while return loss increases within higher frequency bands.

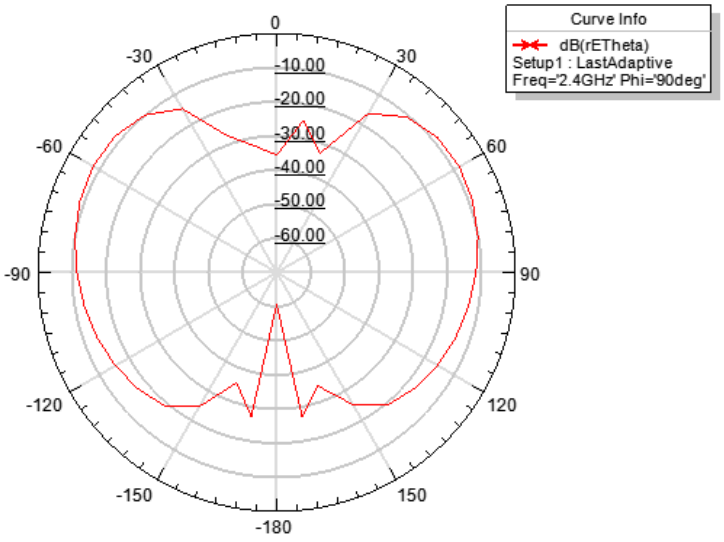

Figure 10: HFSS Circular Ring Patch Antenna E-Plane Co-Pol Radiation Pattern (dB), f = 2.4GHz, φ = 90°, -180° < θ < 180°

Figure 10 presents the Co-Pol E-plane radiation pattern (dB) with fixed φ at 90° and θ swept from -180° to 180°. Radiation patterns were simulated with DGS implemented.

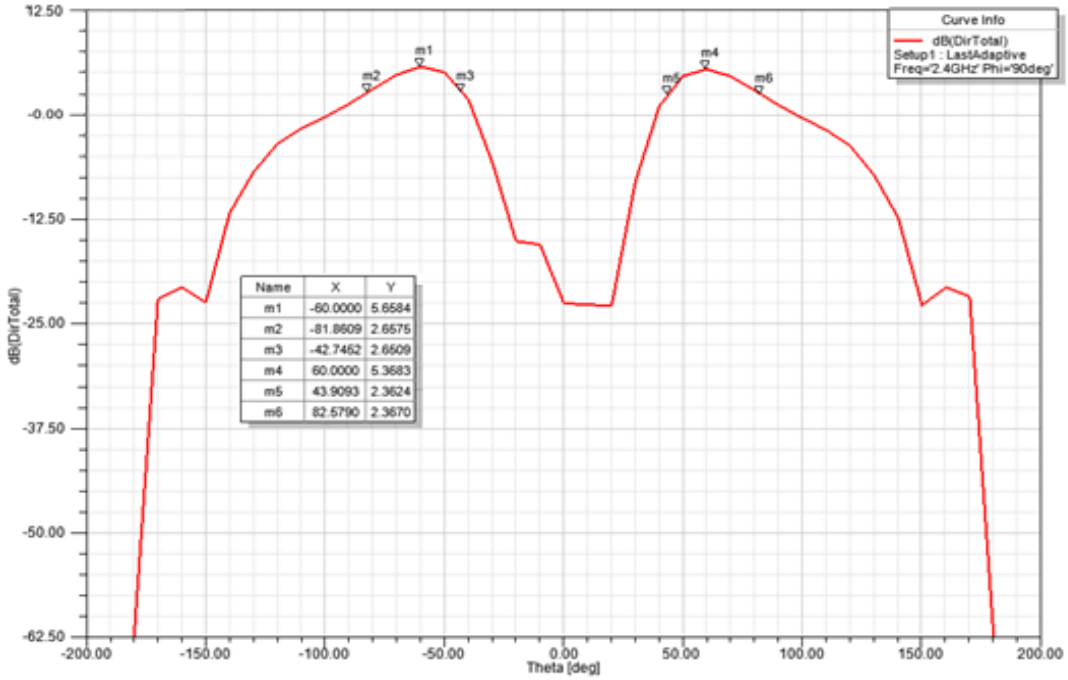

Figure 11: HFSS Circular Ring Patch Antenna Directivity (dB) vs. Frequency (GHz), f = 2.4GHz

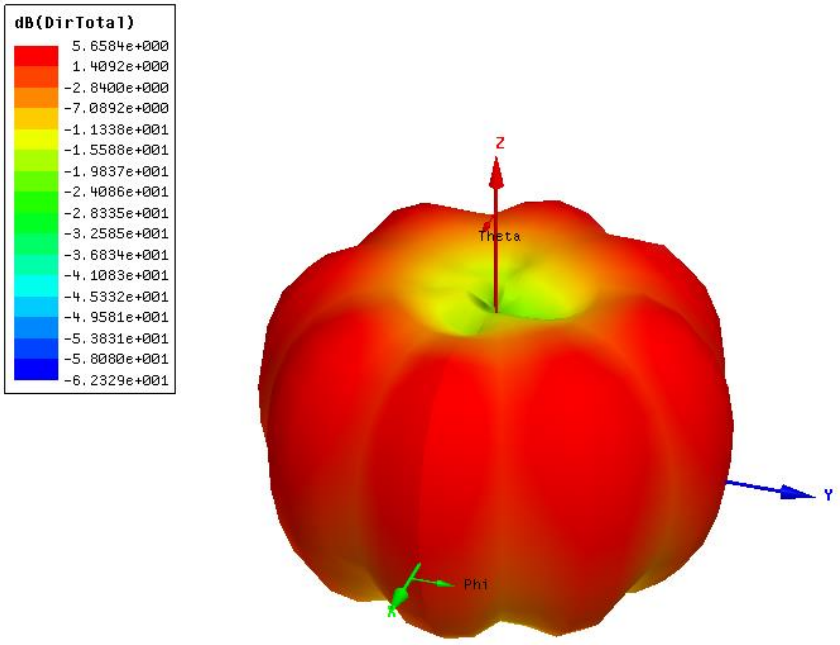

Figure 12: HFSS Circular Ring Patch Antenna Directivity Radiation Pattern (dB), f = 2.4GHz, φ = 90°, -180° < θ < 180° (Above Patch)

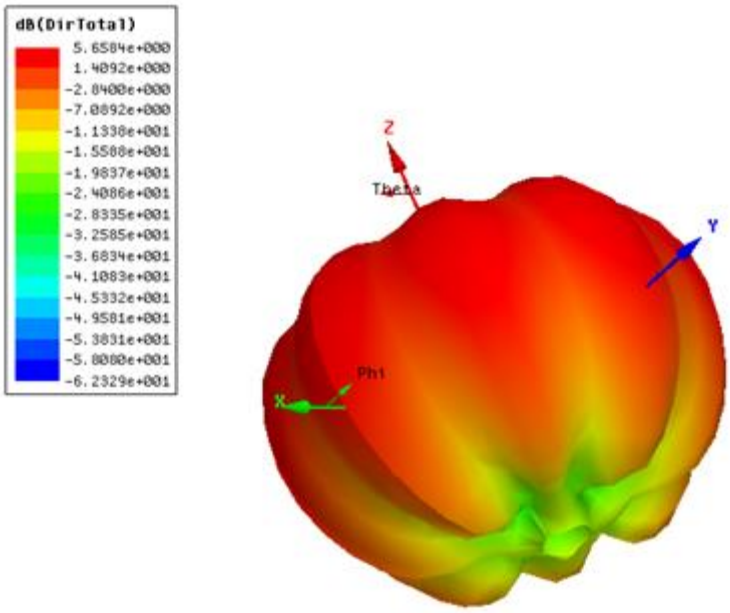

Figure 13: HFSS Circular Ring Patch Antenna Directivity Radiation Pattern (dB), f = 2.4GHz, φ = 90°, -180° < θ < 180° (Below Patch)

Figure 11 shows the directivity frequency response (dB), with maximum 5.7dB directivity, within the typical 5-8dB range for patch directivity. E-plane HPBW is 39°, greater than the expected 36° E-plane HPBW listed in Table III. Figure 12 and Figure 13 display three dimensional directivity radiation patterns (dB) above and below the patch, respectively. The color map in Figure 13 indicates the radiation pattern below the patch has maximum 1.4dB directivity.

IV. SYSTEM TESTING AND RESULTS

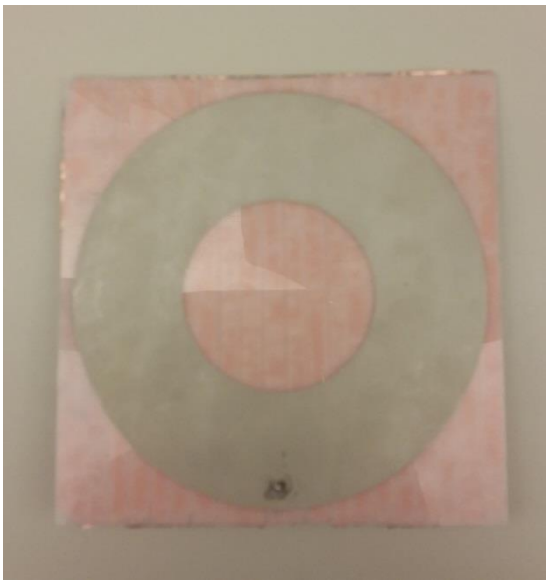

Figure 14: Circular Ring Patch Antenna (Top View)

Figure 15: Circular Ring Patch Antenna (Bottom View)

Figure 14 and Figure 15 show the fabricated circular ring patch antenna and ground layers. The HFSS design from Figure 5 is converted to a .dwg layout for fabrication in the Cal Poly graphic communications electronics screen printing facility. The silver ink circular ring patch is screen printed onto the top layer. Copper foil adhesive tape covers the bottom-side ground plane.

Figure 16: Test Fixture Mounted Circular Ring Patch Antenna in Anechoic Chamber

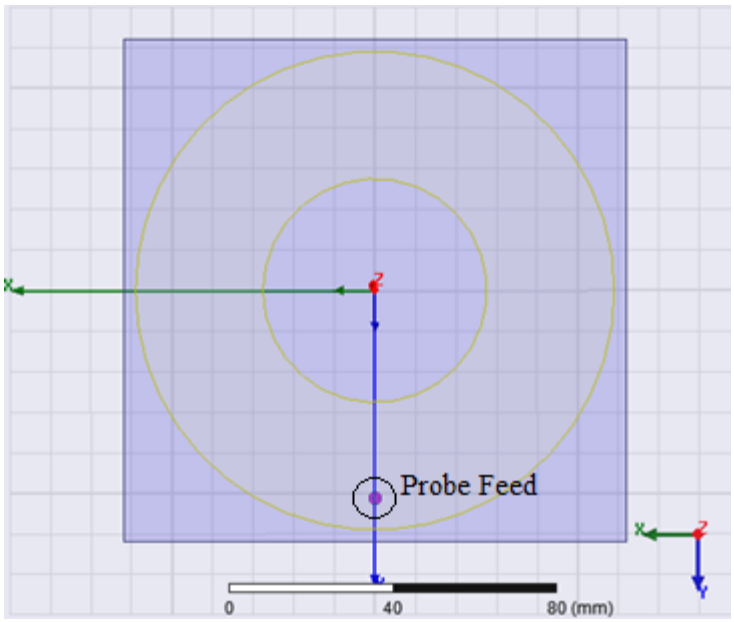

Figure 17: HFSS Coordinate Axes for Test Fixture Mounted Circular Ring Patch Antenna with Probe Feed

Figure 16 shows patch antenna placement in the anechoic chamber. The antenna is mounted to the wood and plastic test fixture. Figure 17 shows the test setup orientation in the HFSS coordinate system. Tests are conducted in the Microwave Laboratory (20-116) anechoic chamber with the Labview AMS software. The anechoic chamber minimizes reflections with RF (radio frequency) absorbent foam interior lining. A standard gain horn antenna transmits toward the receiving patch antenna.

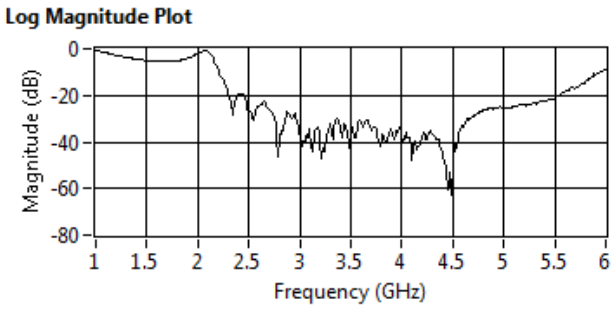

Figure 18: Measured Circular Ring Patch Antenna $|S_{11}|$ (dB) vs. Frequency (GHz)

Figure 18 displays return loss characteristics from 1-6GHz. The 20dB return loss bandwidth includes 2.313-5.550GHz, an 82.335% fractional bandwidth relative to the 3.932GHz center frequency.

Table VII: Measured Circular Ring Patch Antenna $|S_{11}|$ (dB) at WLAN Frequencies

Operating Frequency (GHz)	$\|S_{11}\|$ (dB)	Description
2.313	20.178	Lower 20dB return loss bandwidth frequency bound
2.400	19.661	WLAN designated frequency
3.700	35.256	WLAN designated frequency
5.000	25.314	WLAN designated frequency
5.550	20.489	Upper 20dB return loss bandwidth frequency bound

Table VII lists $|S_{11}|$ points of interest.

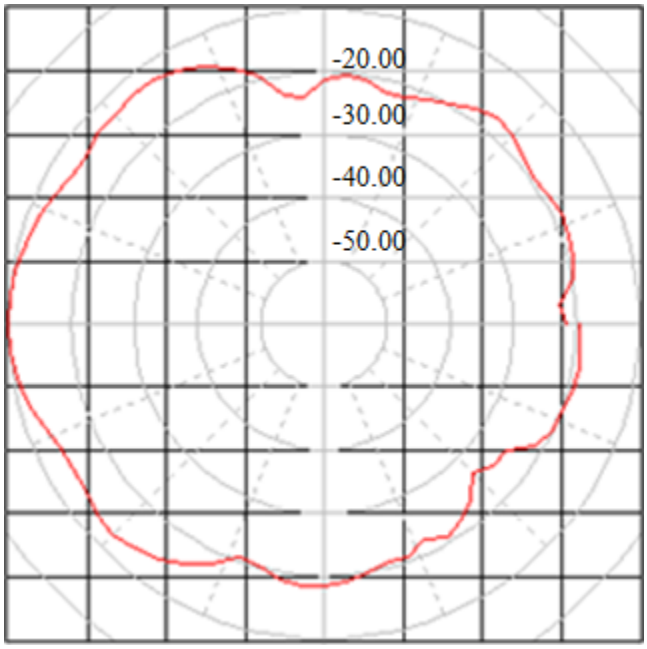

Figure 19: Measured Circular Ring Patch Antenna E-Plane Co-Pol Radiation Pattern (dB), f = 2.4GHz, φ = 90°, -180° < θ < 180°

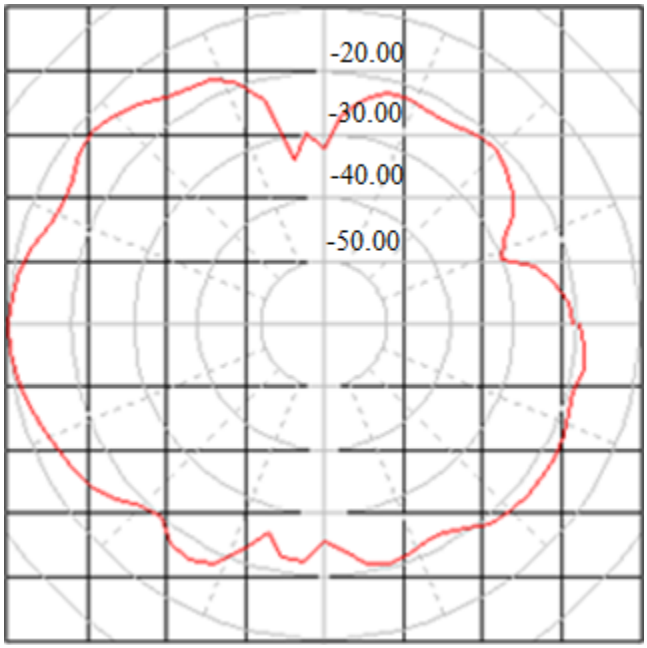

Figure 20: Measured Circular Ring Patch Antenna E-Plane Co-Pol Radiation Pattern (dB), f = 2.7GHz, φ = 90°, -180° < θ < 180°

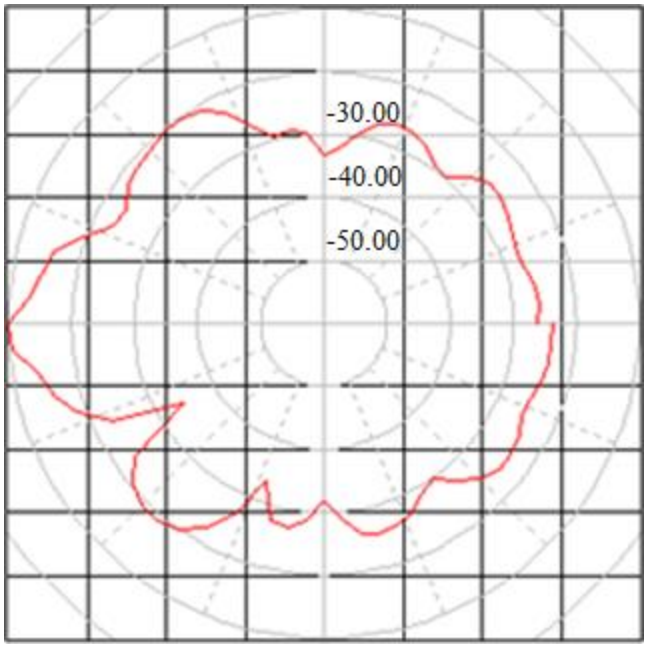

Figure 21: Measured Circular Ring Patch Antenna E-Plane Co-Pol Radiation Pattern (dB), f = 3.1GHz, φ = 90°, -180° < θ < 180°

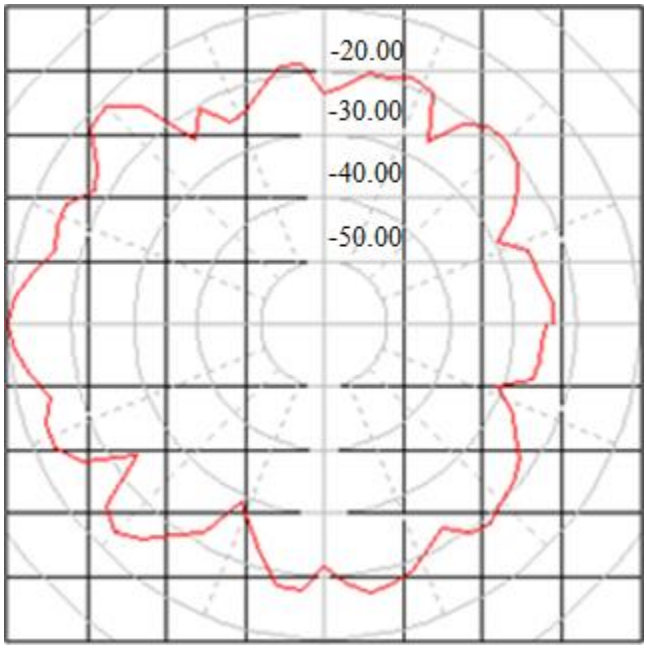

Figure 22: Measured Circular Ring Patch Antenna E-Plane Co-Pol Radiation Pattern (dB), f = 4.6GHz, φ = 90°, -180° < θ < 180°

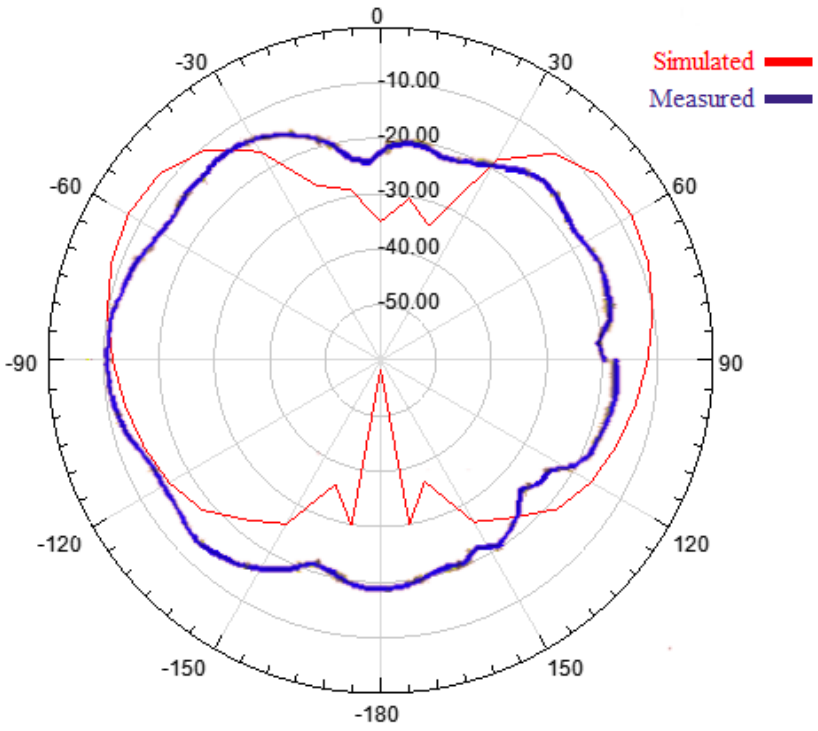

Figure 23: HFSS vs. Measured Circular Ring Patch Antenna E-Plane Co-Pol Radiation Pattern (dB), f = 2.4GHz, φ = 90°, -180° < θ< 180°

Figures 19-22 display E-plane co-polarized radiation patterns (dB) at WLAN operating frequencies. The radiation patterns are directional at the fabricated antenna's resonant frequencies 2.788GHz, 3.213GHz (maximum observed directivity) and 4.488GHz (maximum observed sidelobe level). The radiation pattern at 2.4GHz achieves 7.1dB directivity. Figure 23 overlays measured and simulated radiation patterns at 2.4GHz frequency. Figure 23 indicates the measured radiation pattern has an approximately 40° HPBW from -70° to -110°.

V. CONCLUSION

Table VII lists measured resonant frequencies and corresponding return losses. The fabricated circular ring patch antenna with ground defect achieved 3.237GHz 20dB return loss bandwidth from 2.313-5.550GHz, an 82.335% fractional bandwidth (see Figure 18). Figures 19-22 confirm directional radiation patterns at each WLAN operating frequency. The measured radiation pattern achieves 7.1dB directivity at 2.4GHz. HPBW (E-plane) is approximately 40°.

The measured 20dB return loss bandwidth is 12.033% wider than the target 70.270% fractional bandwidth covering 2.4/3.7/5GHz. Figure 23 compares simulated and measured radiation patterns at 2.4GHz. The measured antenna's 7.1dB directivity is 1.4 ΔdB higher than the simulated maximum 5.7dB directivity. The measured approximate 40° E-plane HPBW is close to the simulated 39° HPBW. The simulated radiation pattern exhibits a null at 180°, which appears to be absent in the measured radiation pattern.

The fabricated and simulated antenna's ground plane differ in terms of ground defect area, shape and deformation such as corrugations in grounding tape, which could lead to discrepancies. A more durable probe feed construction could improve the system. Alternative probe feed connections include embroidery with conductive yarn (less rigid but more durable than solder) and cured conductive epoxy (more rigid than embroidered connections and solder but as brittle as solder). The circular ring patch antenna's operating bandwidth includes unlicensed frequencies from 2.4-5GHz. Notch filters can be designed to prevent illegal bandwidth access.

VI. BIBLIOGRAPHY

1. IEEE Standard for Information Technology, 802.11, 2012.

2. D. M. Pozar and D. H. Schaubert, “Microstrip Antennas: The Analysis and Design of Microstrip Antennas and Arrays,” Hoboken, NJ: Wiley, 1995.

3. R. Kumar and D. C. Dhubarya, “Design and Analysis of Circular Ring Microstrip Antenna,” Global J. of Researches in Eng., vol. 11, no. 1, Feb 2011.

4. L. H. Weng, Y. C. Guo, X. W. Shi, and X. Q. Chen, “An Overview on Defected Ground Structure,” Progress in Electromagnetics Research B. Vol. 7, pp. 173-189, 2008.

5. W. L. Stutzman and G. A. Thiele, “Antenna Theory and Design,” 3rd ed. Hoboken, NJ: Wiley, 2012.

6. B. J. Kwaha, O. N. Inyang, and P. Amalu, “The Circular Microstrip Patch Antenna – Design and Implementation,” University of Jos and Ajayi Crowther University, Jos and Oyo, Nigeria, 2011.

7. K.C. Gupta, “Broadbanding Techniques for Microstrip Patch Antennas – A Review,” University of CO Dept. of Elect. and Comput. Eng., Boulder, CO, Rep. 98, 1988.

APPENDIX A — PARTS LIST AND COSTS

Table VIII: Circular Ring Patch Antenna Materials and Costs

Module	Cost Estimates ($)	Description
Substrate	0.33	124mm x 124mm x 0.3556mm Mylar®/Polyester Film
Patch	5.98	Silver Metal Ink, Conductive Water-Based Coating, 6g, 5 to 6 μm thickness, 8.54 mm^2 coverage area, 33% Ag
Ground	10.34	124mm X 124mm Tapecase Copper Foil Tape
RF Connectors	0.43	1x End Launch PCB Mount SMA Female Plug Straight RF Connector Adapter
Total	17.08	-

Table VIII lists required materials and costs to produce one unit.

APPENDIX B — ANALYSIS OF SENIOR PROJECT DESIGN

1. Summary of Functional Requirements

The fabricated circular ring patch antenna achieves an operating bandwidth that includes 2.4-5GHz WLAN frequencies and 7.1dB directivity at 2.4GHz. The PET substrate is 124mm x 124mm x 0.3556mm (L x W x H). The substrate is thinner than typical microstrip patch antennas ($h < 0.003\lambda$). Antenna size and weight are desirable properties for compact and portable applications. 2.4-5GHz frequency applications include Wi-Fi Internet, Bluetooth (connecting device and peripherals, device synchronization), Zigbee (mesh networking, residential and building controls), industrial processes (self-guided vehicles, communication between machines) and public safety (surveillance, emergency communications).

2. Primary Constraints

Using a lightweight substrate requires design and analysis focused on improving an inherently more narrow impedance bandwidth. Circular ring microstrip patch design and ground defect implementation enables a compact antenna to achieve 2.4-5GHz operating bandwidth.

3. Economic

Human capital includes labor costs. Parts manufacturing, retail and delivery require labor. Substrate production and screen printing processes also require labor. The initial projection based on material costs for producing one antenna is $17.08 (see Table VIII). The projected costs are difficult to estimate because the substrate, ground and RF connectors must be purchased in bulk. Commercial HFSS packages can be accessed in the Microwaves Laboratory (20-116) and cost $50,000. Microwave Laboratory test assets include the Anritsu MS4622B Vector Network Measurement Systems and all anechoic chamber equipment including RF absorbent foam, test fixtures, chamber construction materials and the standard gain horn antenna. The Microwave Laboratory and screen printing facilities require significant overhead expenses and maintenance. Redesign and fabrication caused weeks of delays during project development. Since there is no additional research or redesign prior to manufacturing, approximately one month is required for materials acquisition, fabrication and testing.

4. If Manufactured on a Commercial Basis

Table IX: Circular Ring Patch Antenna Single Unit vs. Bulk Materials and Costs

Module	Single Unit Amount	Bulk Amount	Single Unit Cost Estimates ($)	Bulk Cost Estimates ($)
Substrate	4.882" x 4.882"	3' x 25'	0.33	148.09
Patch	8.54 mm^2	32.77 mm^2	5.98	22.95
Ground	4.882" x 4.882"	1” x 18”	10.34	16.08
RF Connectors	1 unit	20 units	0.43	6.03
Total	-	-	17.08	193.15

Table IX compares single unit and bulk materials and costs. Table VIII lists $17.08 total material costs to produce one unit. Table IX indicates that the product needs to be manufactured and sold in mass quantities for profit. Expenses for manufacturing one unit are over eleven times greater than single unit production costs. Materials such as the RF connectors would cost more individually than if bought in packages containing multiple. Online market research using popular commerce sites (e.g. amazon.com, newegg.com) indicates that Wi-Fi antennas are regularly priced above $40, and assuming each unit requires $17.08 in materials expenses, the project can potentially be marketed alongside other consumer antennas for profit. In order to utilize this product, the user requires a wireless adapter, such as an SMA to USB adapter. There are no additional operating and maintenance costs for the consumer.

5. Environmental

Substrate PET is manufactured in plastic processing plants. Regulated industrial facilities establish safe and efficient environments to limit pollution and material consumption. Recycling plastics is a popular form of environmental conservation in industrial plants. The grounding tape used with the prototype is composed of copper foil cultivated through copper mining. Naturally occurring conductive materials such as copper are depleted as the demand for electronics expands and electronics become more ubiquitous and are manufactured at higher rates. Electromagnetic compatibility standards conformance is unknown without performing certification tests. Used materials, defective parts and waste should be recycled or disposed through electronics waste management facilities.

6. Manufacturability

Screen printing with conductive ink prevents the use of many desirable substrates that could meet

project specifications, such as textiles. Since the patch antenna is fabricated using precision screen printing, inaccuracies in attaining the simulated model's dimensional specifications or using conductive ink deposition and curing are not an issue. Grounding tape deforms easily and corrugations may cause unwanted effects and involves unnecessary labor and costs to implement, hence, screen printing the ground plane as an alternative is favorable.

7. Sustainability

Performance errors caused by deformation over long periods of time in portable applications were not experimentally studied due to the relatively short project time frame. The probe feed coaxial connection is constructed using rigid yet brittle solder. Alternative feed configurations using embroidered or cured epoxy connections could potentially enhance the feed connection's durability and extend the product's lifetime. Implementing design improvements entails another fabrication and testing cycle, requiring more time, labor and materials and hence more costs. The 124mm x 124mm plastic antenna consumes relatively little material because of its compact dimensions. Required materials are plastic (substrate), copper (adhesive tape) and silver (conductive ink).

8. Ethical

The product can potentially be used to access unlicensed bands specified in the IEEE 802.11 protocols. Notch filters that eliminate access to specific frequencies can be configured on the patch to prevent this issue.

9. Health and Safety

Electromagnetic interference issues including emissions, immunity and signal integrity were not tested according to standards for regulatory compliance. Noncompliance results in product performance degradation, adverse effects on other electronics and human exposure to unsafe levels of emissions.

10. Social and Political

Social impacts of the device include wireless congestion due to increased widespread WLAN access. The 2.4GHz frequency band in particular has become so congested that 5GHz and 5.9GHz are being used more frequently to allocate bandwidth for 2.4GHz applications. The product impacts wireless service providers as their services are used more heavily. The antenna's use can lead to signal congestion in crowded networks, due to RF interference. Interference causes network slowdowns due to the antenna's inability to distinguish signals and packet loss followed by reconnection attempts. This affects both the provider's service quality and the user's experience.

11. Development

Information available through the IEEE Xplore Digital Library provides insights into patch antenna theory and design and has proved invaluable to project development. Familiarization with procedures and test equipment used for antenna measurements such as anechoic chamber measurements became indispensable knowledge. HFSS design and analysis enriched an understanding of a powerful tool that is prevalent in the RF industry.